Ag, Ge dual gradient substitution for Low-Energy Loss and High Efficiency Kesterite Solar Cells

Junjie Fu, Dongxing Kou*, Wenhui Zhou, Zhengji Zhou, Shengjie Yuan, Yafang Qi, and Sixin Wu*

Key Lab for Special Functional Materials, Ministry of Education, National & Local Joint Engineering Research Center for High-Efficiency Display and Lighting Technology, School of Materials Science and Engineering, Collaborative Innovation Center of Nano Functional Materials and Applications, Henan University, Kaifeng 475004, China.

E-mail: koudongxing@henu.edu.cn; wusixin@henu.edu.cn.

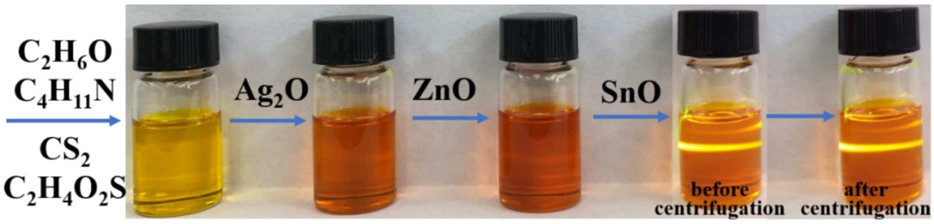

Fig. S1 The typical operation procedures for the preparation of AZTS precursor solution.

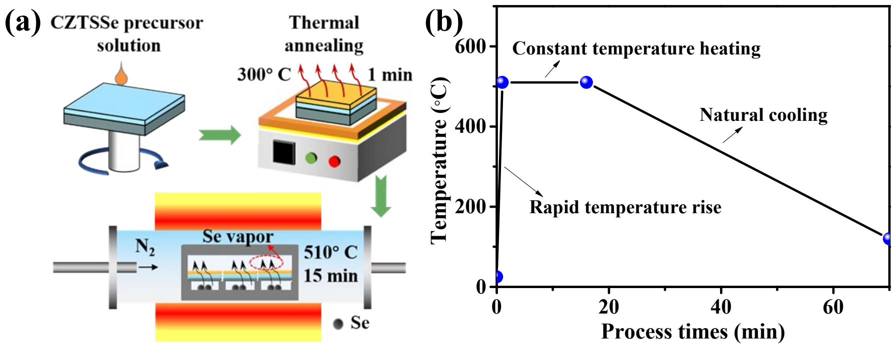

Fig. S2 (a) Schematic diagram of annealing procedure for selenized CZTSSe films and (b) the corresponding temperature duration of each step.

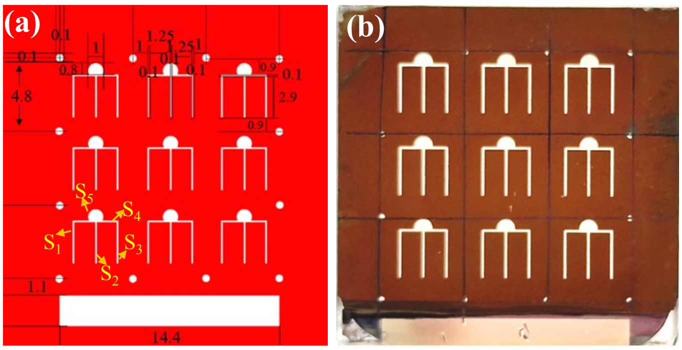

Fig. S3 (a) Template drawings and (b) digital photograph of the fabricated CZTSSe solar cells. The unit in (a) is mm and the total area of the solar cell is 0.2304 cm^2. After minus the silver grid area of S_1 (0.0029 cm^2), S_2 (0.0029 cm^2), S_3 (0.0029 cm^2), S_4 (0.0028 cm^2) and S_5 (0.0068 cm^2), the effective area is 0.2121 cm^2 for the fabricated device.

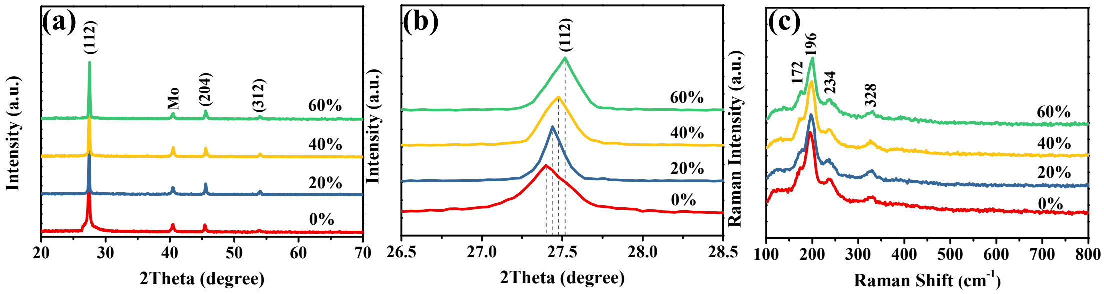

Fig. S4 (a) X-ray diffraction spectra, (b) enlarged view of the (112) peaks, and (c) Raman spectra of the selenized single Ge gradient CZTSSe thin films with different bottom Ge/(Sn+Ge) ratios.

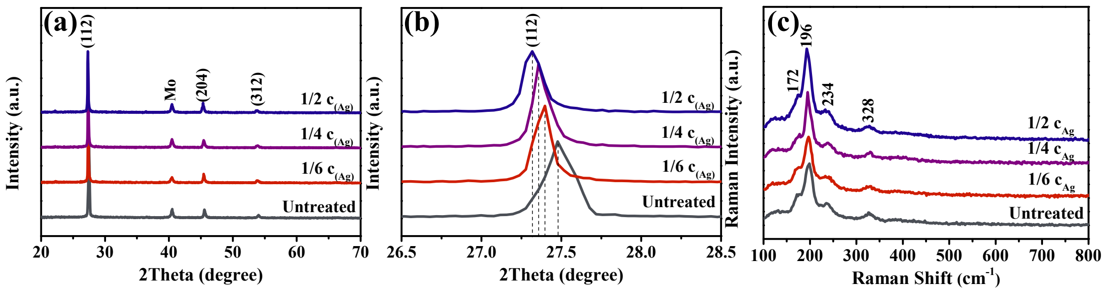

Fig. S5 (a) X-ray diffraction spectra, (b) enlarged view of the (112) peaks, and (c) Raman spectra for the selenized Ag, Ge dual gradient CZTSSe thin films with different diluted AZTS concentration (untreated, 1/6, 1/4, 1/2 c_{Ag}) on top of the 40% Ge gradient CZTSSe films.

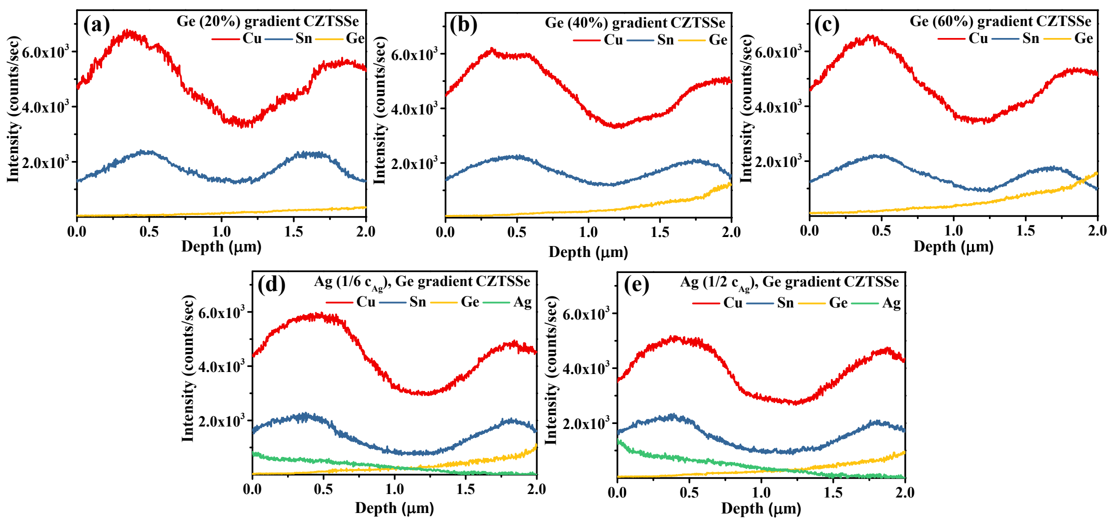

Fig. S6 SIMS depth profiles of Cu, Sn, Ag and Ge element throughout (a-c) the independent Ge gradient and (d-e) Ag, Ge dual gradient samples with different substitution contents. The scan direction is from surface absorber towards Mo substrate.

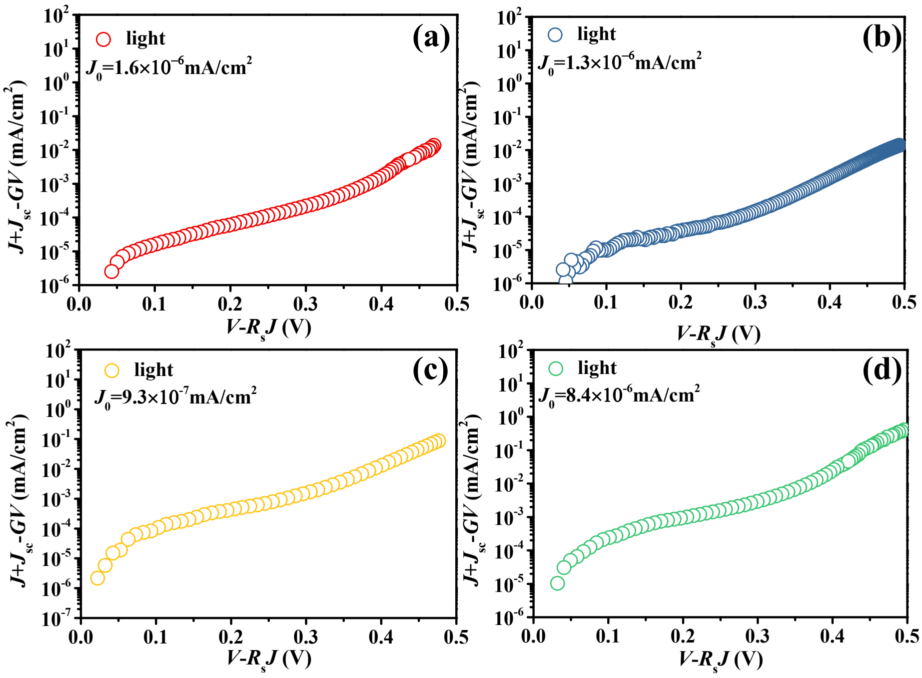

Fig. S7 Semi-logarithmic plots of J+J_{sc}-GV vs V-R_sJ for Ge gradient CZTSSe devices with different Ge/(Ge+Sn) ratio: (a) 0%, (b) 20%, (c) 40%, and (d) 60%. J_0 is obtained from the intercept of linear region.

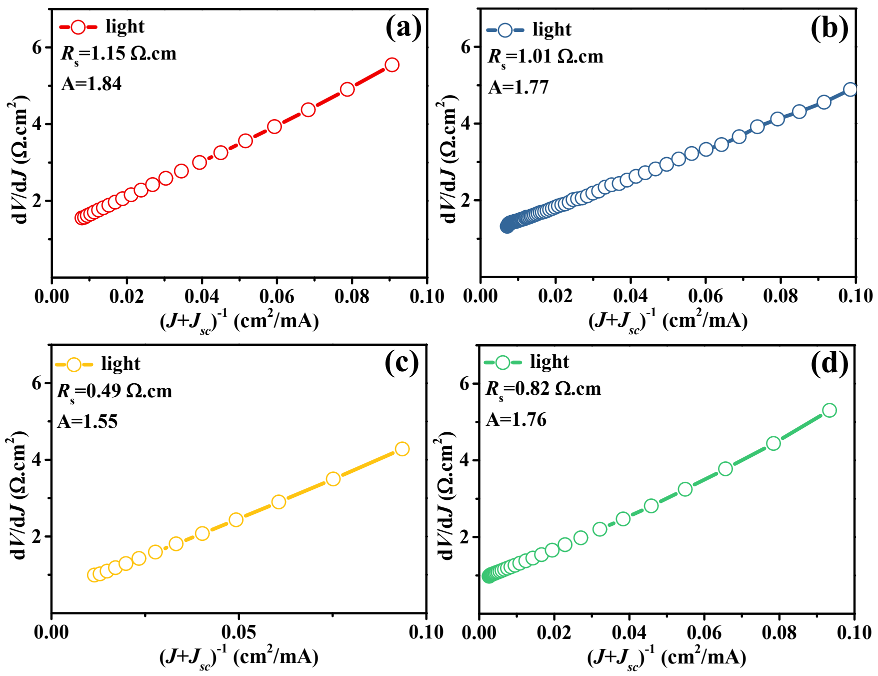

Fig. S8 dV/dJ vs (J+J_{sc})$^{-1}$ curves for Ge gradient CZTSSe divices with different Ge/(Ge+Sn) ratio: (a) 0%, (b) 20%, (c) 40%, and (d) 60%. R_s is obtained from the intercept of linear region, and the slope is equal to AkT/q, where q/kT=38.7.

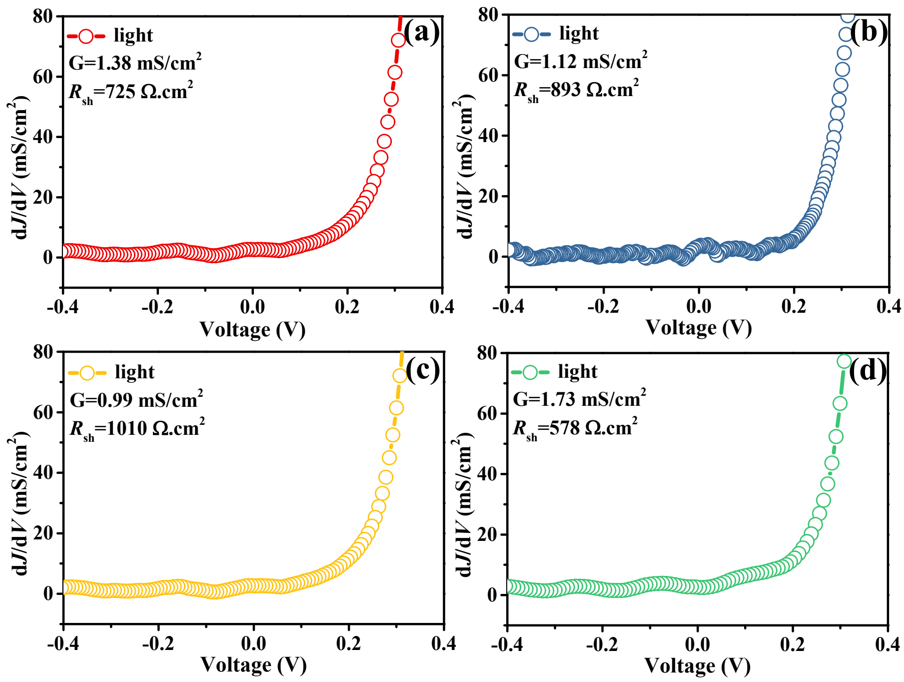

Fig. S9 dJ/dV vs V curves for Ge gradient CZTSSe devices with different Ge/(Ge+Sn) ratio: (a) 0%, (b) 20%, (c) 40%, and (d) 60%. G_{sh} is evaluated from the average value of plateau range (-0.2~0.2 V), and its reciprocal represents R_{sh}.

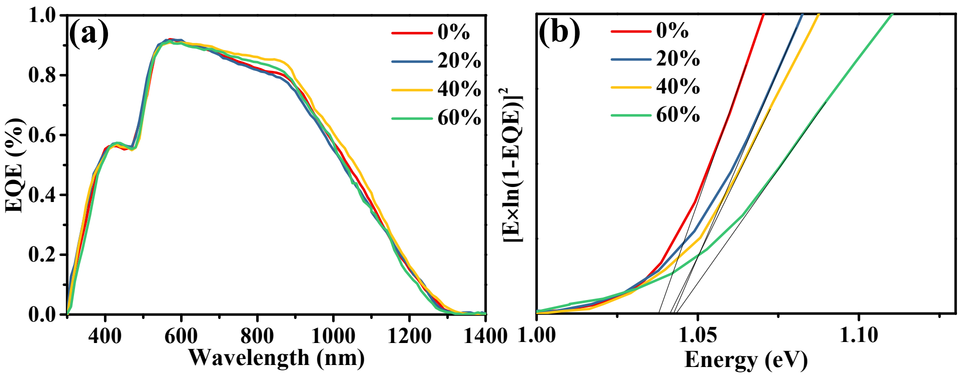

Fig. S10 (a) EQE curves and (b) the extracted band gap of Ge gradient CZTSSe absorbers with different bottom Ge content.

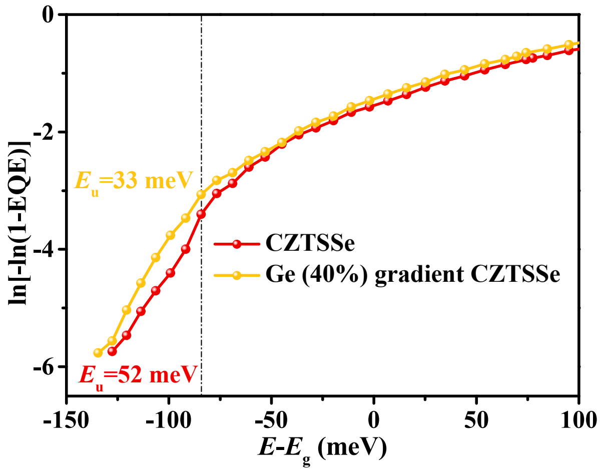

Fig. S11 Urbach tail energies (E_u) extracted from ln[-ln(1-EQE)] vs E-E_g for the reference and 40% Ge gradient CZTSSe devices

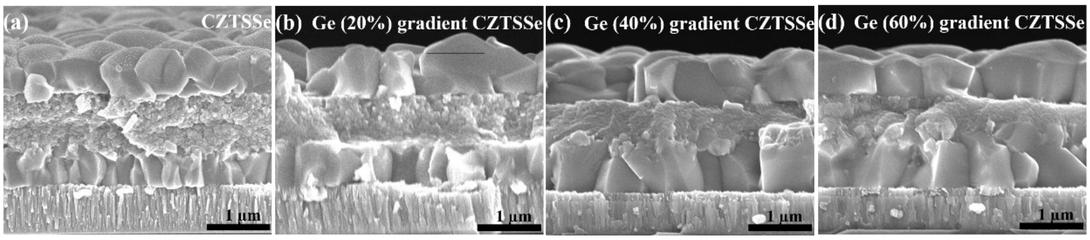

Fig. S12 The cross-section SEM images of CZTSSe absorber with different Ge substitution content in the bottom layers.

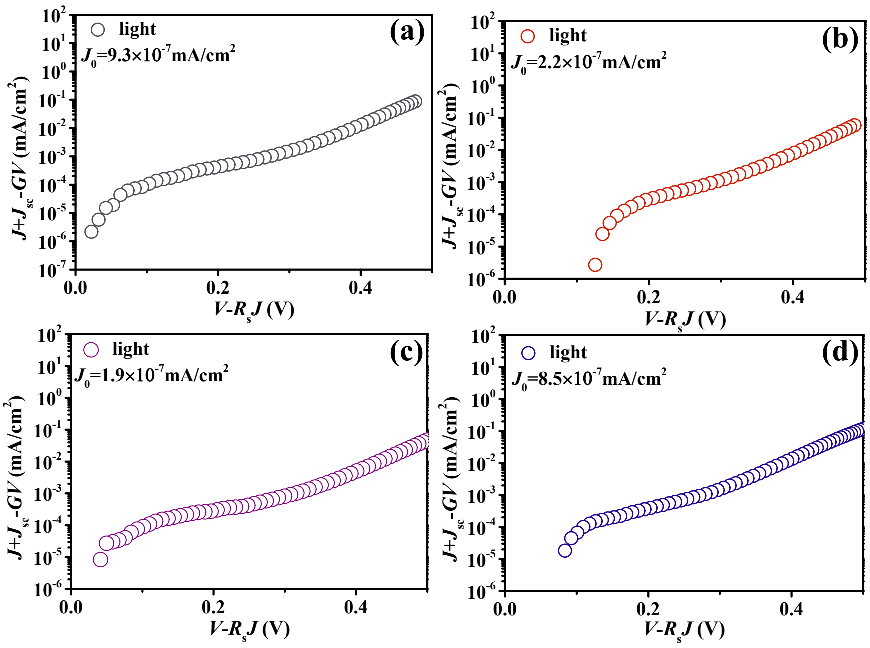

Fig. S13 Semi-logarithmic plots of J+J_{sc}-GV vs V-R_sJ for Ag, Ge dual gradient CZTSSe devices with different diluted AZTS concentration on top of the 40% Ge gradient films: (a) untreated, (b) 1/6, (c) 1/4, and (d) 1/2 c_{Ag}. J_0 is obtained from the intercept of linear region.

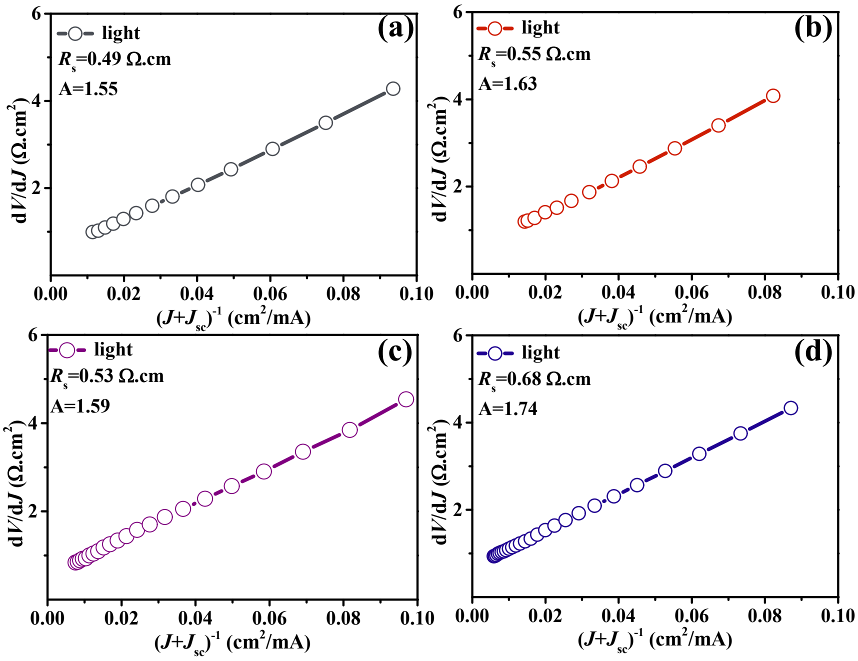

Fig. S14 dV/dJ vs $(J+J_{sc})^{-1}$ curves for Ag, Ge dual gradient CZTSSe devices with different diluted AZTS concentration on top of the 40% Ge gradient films: (a) untreated, (b) 1/6, (c) 1/4, and (d) 1/2 c_{Ag}. R_s is obtained from the intercept of linear region, and the slope is equal to AkT/q, where q/kT=38.7.

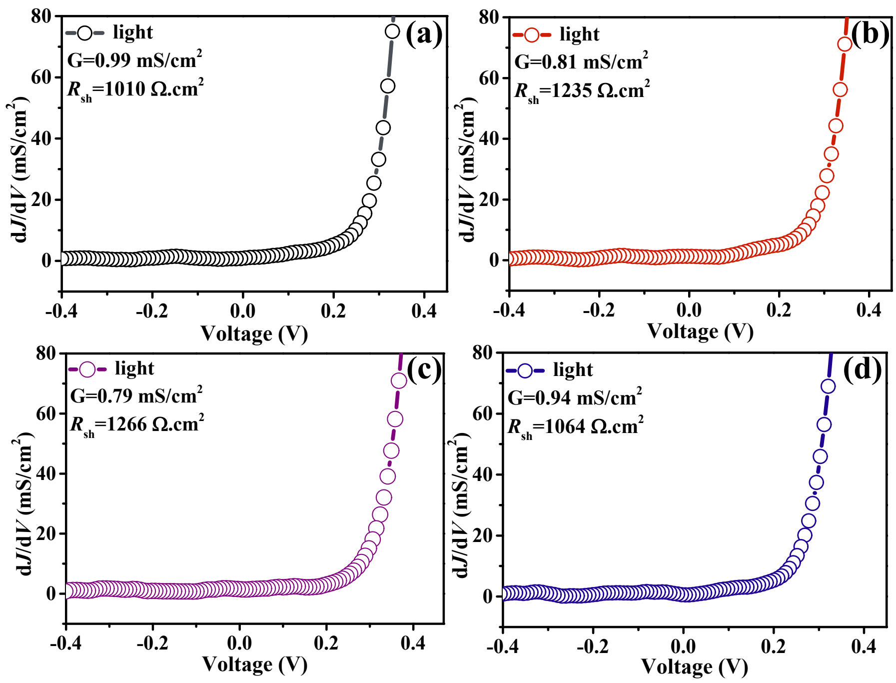

Fig. S15 dJ/dV vs V curves for Ag, Ge dual gradient CZTSSe devices with different diluted AZTS concentration on top of the 40% Ge gradient films: (a) untreated, (b) 1/6, (c) 1/4, and (d) 1/2 c_{Ag}. G_{sh} is evaluated from the average value of plateau range (-0.2~0.2 V), and its reciprocal represents R_{sh}.

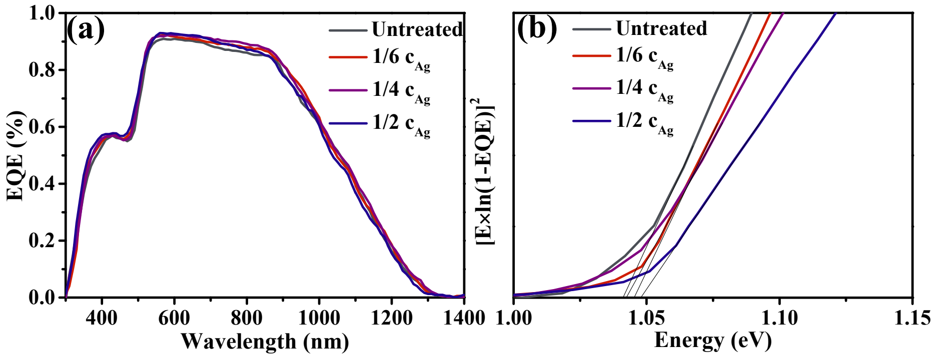

Fig. S16 (a) EQE curves and (b) the extracted band gap of Ag, Ge dual gradient CZTSSe absorbers with different diluted AZTS concentration on top of the 40% Ge gradient films.

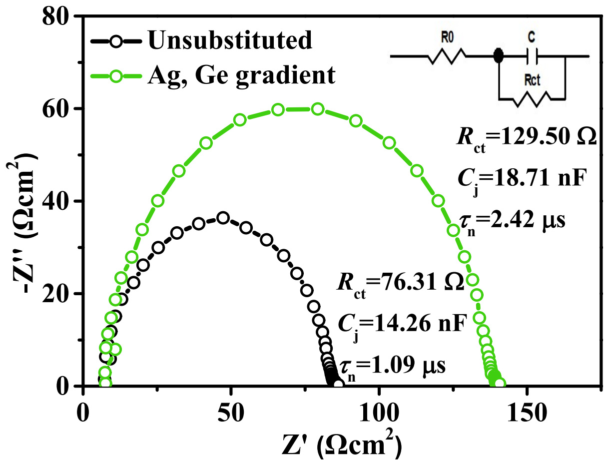

Fig. S17 EIS Nyquist plots of unsubstituted and Ag, Ge dual gradient CZTSSe solar cells at -0.4 V bias. Insert is the equivalent circuit.

Table S1 EDX data of the Ge gradient CZTSSe absorbers derived from random selected sites in SEM cross-section.

Position	S(%)	Cu(%)	Zn(%)	Ge(%)	Se(%)	Sn(%)	Ge/(Sn+Ge) (%)
A	8.79	19.75	13.36	0.16	48.54	9.4	1.67
B	9.87	20.23	13.62	0.18	46.86	9.24	1.91
C	8.45	19.89	14.82	0.35	46.56	9.93	3.39
D	9.14	18.52	13.31	0.29	49.38	9.36	3.01
E	9.62	6.15	6.73	0.42	70.94	6.14	6.4
F	10.34	6.32	7.59	0.45	69.48	5.82	7.18
G	8.64	17.21	13.15	1.11	52.18	7.71	12.58
H	9.18	18.46	14.73	1.24	47.74	8.65	12.54
I	9.69	17.71	13.27	2.25	50.07	7.01	24.3
J	8.95	17.35	13.34	2.18	51.13	6.95	23.88